

New Constraints on Higgs-Portal Scalar Dark Matter

Huayong Han and Sibozheng

Department of Physics, Chongqing University, Chongqing 401331, P.R. China

Abstract

The simplest Higgs-portal dark matter model, in which a real scalar singlet is added to the standard model, has been comprehensively revisited, by taking into account the constraints from perturbativity, electroweak vacuum stability in the early Universe, dark matter direct detection, and Higgs invisible decay at the LHC. We show that the *resonant mass region* is totally excluded and the *high mass region* is reduced to a narrow window $1.1 \text{ TeV} \leq m_s \leq 2.55 \text{ TeV}$, which is slightly reduced to $1.1 \text{ TeV} \leq m_s \leq 2.0 \text{ TeV}$ if the perturbativity is further imposed. This *high mass region* can be fully detected by the Xenon1T experiment.

1 Introduction

The Standard Model (SM) as the effective theory below the electroweak (EW) scale has been established after the discovery of SM Higgs scalar with mass around 125 GeV [1, 2] at the Large Hadron Collider (LHC). Unfortunately, there is no viable candidate for a dark matter (DM) in the SM, which implies that an extension beyond the SM is necessary.

Among viable extensions the simplest Higgs-portal dark matter (HDM) [3, 4, 5, 6, 7] is the most economic and of special interest from both the DM- and LHC-phenomenology. In this extension, only a real singlet scalar s is added to the SM. With the aid of Z_2 parity which is needed for the stability of singlet DM, the number of model parameters is reduced to three. It implies that the minimal model is very predictable. In the subsequent studies on the HDM [8, 9, 10, 11, 12, 13, 14, 15, 16, 17, 18, 19, 20, 21], the parameter space is analyzed in terms of experimental constraints as follows.

- Dark matter relic density [22], which shows that the *low mass region*, *resonant mass region*, and *high mass region* are all viable.
- Dark matter direct detection such as Xenon100 [23], Xenon1T [24] and LUX [25] experiments, which are able to effectively detect the *high mass region* up to ~ 3 TeV.
- Limit on the Higgs invisible decay $h \rightarrow ss$, which can effectively detect the *low mass region* with m_s of order a few GeV.
- Indirect detection such as limit on γ -ray lines from the Fermi-LAT [27] is rather efficient to constrain the *resonant mass region* [28, 29, 30].

However, these constraints are not sufficient, as some possibly strong theoretic ones have been ignored. The object of this paper is to take into account all known experimental and theoretic constraints. Simultaneously, experiments constraints will be updated, if available. In compared with the previous works, e.g., a comprehensive review in [21], our main differences are the following ones.

- The SM EW vacuum suffers from large quantum fluctuations in the early Universe as induced by the inflation, which imposes *strong* constraint [32, 33, 34] on the model parameters. SM vacuum stability must be taken into account to constrain the parameter space. For an earlier attempt, see [35, 36].

- Assume the HDM as an effective theory between the EW and Plank scale, perturbative analysis should be considered seriously, which leads to *strong* upper bounds on the quartic coupling constant of $s^2 |H|^2$ and the DM self-coupling constant. This effective theory can be applied, e.g., to S-inflation, where the scalar singlet DM is identified as the inflaton [37].
- Very recently, the ATLAS collaboration has reported the latest limit about the Higgs invisible decay width [26] in the low and resonant mass regions. This will be updated in our analysis.

The paper is organized as follows. In Sec.2, we introduce notation and conventions in the HDM. In this section the constraint on the model parameters from the requirement of perturbativity is studied. In Sec.3, we discuss the constraint on the model parameters from the SM vacuum stability for 125 GeV Higgs mass. No additional mechanism for stabilizing the SM vacuum stability is employed except the DM scalar.

In Sec.4 we re-examine the DM phenomenology. In particular, we calculate the s scalar relic density and the spin-independent nucleon-DM scattering cross section by using MicrOMEGAs [38], which are consistent with results in some earlier literature. In Sec.5, we update the LHC phenomenology about scalar DM, by focusing on the latest limit on the Higgs invisible decay.

Finally, we present our main conclusions in Sec.6. We find that the *resonant mass region* is totally excluded and the *high mass region* is reduced to a narrow window $1.1 \text{ TeV} \leq m_s \leq 2.4 \text{ TeV}$. If the requirement of perturbativity is further imposed, the allowed mass range is slightly reduced to $1.1 \text{ TeV} \leq m_s \leq 2.0 \text{ TeV}$. In either case the mass window can be fully detected by the Xenon 1T experiment.

2 HDM within Perturbative Region

The Lagrangian for the simplest HDM with a Z_2 parity, under which s is odd and SM particles are even, is given by,

$$\mathcal{L} = \mathcal{L}_{\text{SM}} + \frac{1}{2} (\partial s)^2 + V(s, H) \quad (2.1)$$

where

$$V(s, H) = \frac{\lambda}{2} \left(|H|^2 - \frac{v^2}{2} \right)^2 + \frac{\mu_s^2}{2} s^2 + \frac{\lambda_s}{2} s^4 + \frac{\kappa_s}{2} s^2 |H|^2. \quad (2.2)$$

In Eq.(2.2) the first term denotes the Higgs potential with EW scale $v \simeq 246$ GeV, and the λ_s -term and κ_s -term refers to s self-interaction and Higgs-DM interaction, respectively. Expand the fields as $H = (v + h)/\sqrt{2}$ and $s = \langle s \rangle + s = 0 + s$ along the vacuum structure for positive λ_s and κ_s ¹, one obtains from Eq.(2.2),

$$V(s, h) = \frac{1}{2}m_s^2 s^2 + \frac{\lambda_s}{2}s^4 + \frac{\kappa_s v}{2}s^2 h + \frac{\kappa_s}{4}s^2 h^2. \quad (2.3)$$

where $m_s = \mu_s^2 + \kappa_s v^2/2$. Remarkably, there are only three new parameters in the HDM. It implies that this model can be studied concretely.

In some situations perturbativity should be imposed on the model. This is true when it is assumed to the effective theory below some high energy scale such as Plank mass scale. See, e.g. [37] for an application of such idea to the S-inflation.

In Fig.1 we show the upper bounds on the EW values of κ_s and λ_s by the requirement of perturbativity

$$0 < \kappa_s(\mu) < \sqrt{4\pi}, \quad 0 < \lambda_s(\mu) < \sqrt{4\pi}, \quad (2.4)$$

for Renormalization Group (RG) scale μ between the EW and Plank mass scale. We have used two-loop RG equations [41],

$$\begin{aligned} \beta_{\kappa_s} &= \frac{1}{(4\pi)^2} \left[- \left(\frac{9}{10}g_1^2 + \frac{9}{2}g_2^2 - 6\lambda - 6y_t^2 - 12\lambda_s \right) \kappa_s + 4\kappa_s^2 \right] + \frac{1}{(4\pi)^4} \cdots \\ \beta_{\lambda_s} &= \frac{1}{(4\pi)^2} (\kappa_s^2 + 36\lambda_s^2) + \frac{1}{(4\pi)^4} \cdots \end{aligned} \quad (2.5)$$

where g_i refer to the SM gauge coupling, and y_t denotes the top Yukawa coupling. As expected from Eq.(2.5), the correlation between the upper bounds on κ_s and λ_s is mildly sensitive to s scalar mass, but strongly to each other. Our scan shows that the critical values are given by $\kappa_s < 0.6$ and $\lambda_s < 0.131$.

Of course, these bounds can be relaxed when the high energy scale above which the model is not effective is smaller than our reference value.

¹The vacuum is given by $\langle H \rangle = v/\sqrt{2}$ and $\langle s \rangle = 0$ for both positive λ_s and κ_s , which may be violated when both of them are negative. However, as we will shown in Sec.3, neither negative κ_s and nor negative λ_s are favored by the EW vacuum stability. In this paper we choose both positive λ_s and κ_s for our discussion.

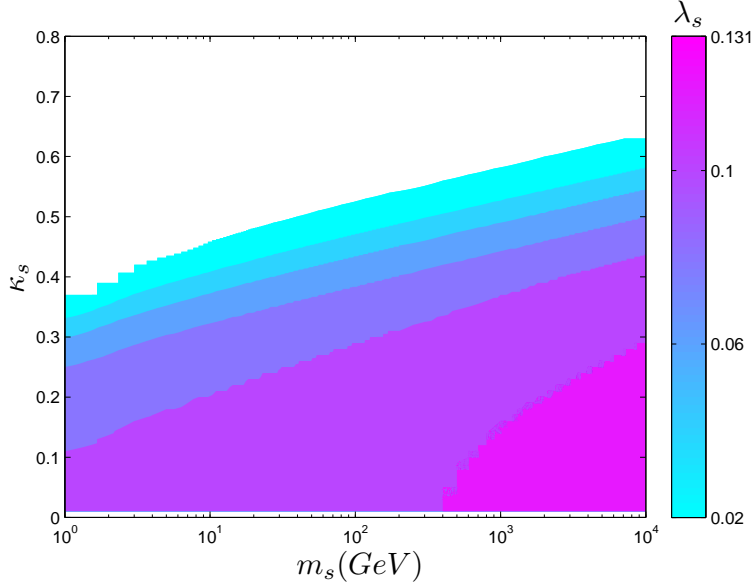


Figure 1: Upper bounds on the EW values of κ_s and λ_s from the requirement of perturbativity below the Plank scale.

3 Electroweak Vacuum Stability

It was shown in [31] that the EW vacuum is metastable for the observed Higgs mass $m_h \simeq 125$ GeV, as seen from the RG equation for λ . Since the sign of beta function β_λ is always negative in the SM, λ becomes negative above some critical RG scale μ_* . μ_* is approximately equal to the value h_* , at which the Higgs potential is maximal. For the central values of top quark mass $m_t = 173.2$ GeV and structure constant of QCD gauge coupling $\alpha = 0.1184$, $h_* \simeq 10^9 - 10^{10}$ GeV at the two-loop level. The situation can be improved to $h_* \simeq 10^{19}$ GeV for lighter m_t within 1σ uncertainty [42]. So, in the most of SM parameter space EW vacuum is only metastable.

For EW vacuum being metastable, it suffers from large quantum fluctuation in the early Universe, especially during and after inflation, which leads to strong theoretic constraint on the model parameters.

Let us firstly discuss the survival probability of EW vacuum during inflation. Denote $P(h, t)$ the probability for Higgs field with the value h at time t , which can be determined via solving the Fokker-Plank equation [32, 33, 34],

$$\frac{\partial P}{\partial t} = \frac{\partial}{\partial h} \left[\frac{H_c^3}{8\pi^2} \frac{\partial P}{\partial h} + \frac{V'(h)}{3H_c} P \right]. \quad (3.1)$$

Here H_c refers to the Hubble parameter², which is approximate constant during inflation. V' denotes derivative of Higgs potential over Higgs field. For the case $h < h_*$ the quantum fluctuation- H_c^3 term dominates the classical one-the last term in Eq.(3.1). If one ignores this classical term, Eq.(3.1) can be easily solved in terms of separating variants and resonable boundary conditions. See [33, 34] for details. Then, the probability for staying at the domain $h > h_*$ other than EW vacuum at the end of inflation is given by,

$$P(|h| > h_*) = 1 - \int_{-h_*}^{h_*} P(h, \frac{N}{H_c}) dh, \quad (3.2)$$

where $N \simeq 55 - 60$ is the number of e-folds.

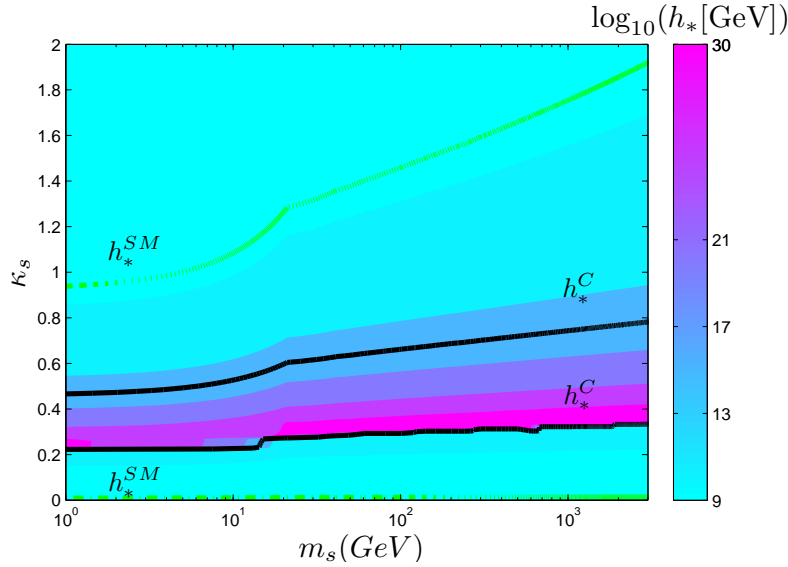


Figure 2: The value of h_* at which the Higgs potential is maximal in the parameter space of $\kappa_s - m_s$. The green curves correspond to the case of SM. The black curves show the critical value as required by EW vacuum stability. It clearly shows that the value of h_* can be uplifted into the region surrounded by the two black curves.

If the probability for staying at the metastable EW vacuum is not zero as required, $P(|h| > h_*)$ should be smaller than e^{-3N} , which gives rise to,

$$h_* > \sqrt{\frac{3}{2}} \frac{N}{\pi} H_c \simeq 25 H_c \simeq 2.5 \times 10^{17} \text{ GeV}. \quad (3.3)$$

²The magnitude of Hubble constant is directly related to the scalar-to-tensor ratio r , with $H_c \simeq 1 \times 10^{16} \times (r/0.01)^{1/4}$ GeV. We take $H_c = 10^{16}$ GeV as the reference point, which is a good approximation unless r is extremely small.

Obviously, this condition cannot be satisfied in the most of parameter space of SM. The constraint in Eq.(3.3) can be relaxed in the context of SM by introducing a new interaction $\xi_H \mathcal{R}^2 |H|^2$ [34, 43] between the Higgs and Ricci scalar \mathcal{R} .

With no need of parameter ξ_H , this reduction can be alternatively realized in the HDM. It is easy to understand in terms of the new contribution to beta function β_λ , which reads at the two-loop level,

$$\delta\beta_\lambda = \beta_\lambda^{(\text{HDM})} - \beta_\lambda^{(\text{SM})} = \frac{\kappa_s^2}{(4\pi)^2} + \frac{1}{(4\pi)^4}(-5\lambda\kappa_s^2 - 4\kappa_s^3). \quad (3.4)$$

The value of h_* can be uplifted for small κ_s , as the sign of the new contribution in Eq.(3.4) can be positive in this region. In contrast, h_* may be reduced in the region of large κ_s , where the sign of the new contribution in Eq.(3.4) is negative. The green curve in Fig.2 clearly shows the critical value $\kappa_s^c \sim 0.9$ ³. Below this critical value h_* can be larger than SM value h_*^{SM} . More interesting, as shown by the red region corresponding to the range $\kappa_s \simeq 0.25 - 0.8$, the required value $h_*^c = 2.5 \times 10^{17}$ GeV in Eq.(3.3) can be satisfied.

The effect on the vacuum stability of the singlet scalar potential due to quantum fluctuations is more easily understood, in comparison with the Higgs potential. Since $\langle s \rangle = 0$ is the true minimal of singlet scalar potential, quantum fluctuation with magnitude of order $\delta s \sim H_c$ may push s towards to an unstable vacuum from the origin. But it rapidly returns to the origin vacuum through classical tunnelling process. This understanding holds as long as λ_s is always positive between the EW and Plank scale.

Once inflation ends, (p)reheating begins immediately. The quantum effect on the EW vacuum during (p) reheating can be studied in terms of the equations of motion for s and Higgs in principle. Unfortunately, a concrete constraint on the model parameters in HDM can not be derived without knowledge of reheating temperature T_{re} , which is an important physical quantity involved [34]. To determine T_{re} interactions between the inflaton scalar and SM fields should be given explicitly.

4 Dark Matter Phenomenology

In this section we firstly consider the constraints arising from the DM relic density and direct detection limits at the LUX and Xenon100 experiments. Then we discuss the prospect at the Xenon1T experiments.

³For negative κ_s , $|\kappa_s^c|$ is larger in comparison with positive κ_s . However, its magnitude is more seriously bounded above by the analysis of perturbativity.

4.1 Relic Density

The Plank and WMAP 9-year data have measured the DM relic density in high precision [22],

$$\Omega_{\text{DM}} h^2 = 0.1199 \pm 0.0027 \quad (4.1)$$

With the assumption that the relic density of s scalar is totally produced by the thermal freeze-out process, we have

$$\Omega_s h^2 \sim 0.1 \text{ pb} / \langle \sigma_{\text{ann}} v \rangle$$

where σ_{ann} is the total annihilation cross-section for s and v is the relative velocity.

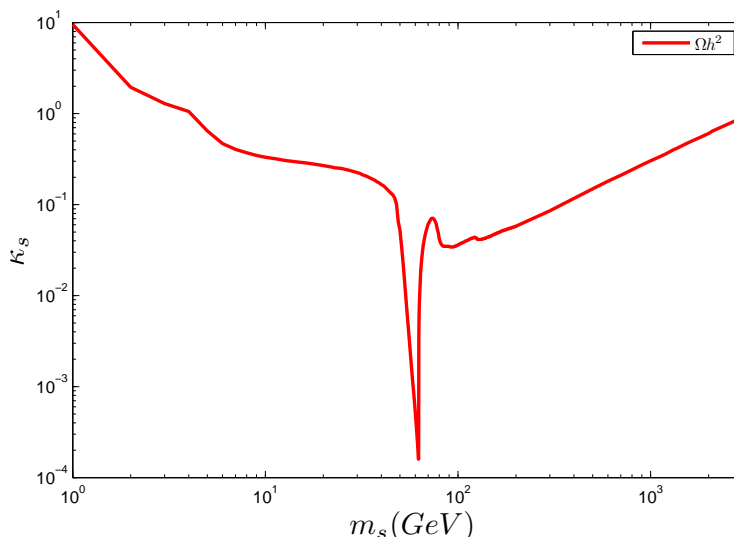


Figure 3: Contours of s scalar relic density $\Omega_s h^2$ as required by the DM projected to the two-parameter plane of (m_s, κ_s) .

The ss annihilation mainly proceeds through Higgs-mediated process in the s channel. Sub-dominant process include s exchange in the t channel and annihilation into hh . So, σ_{ann} is sensitive to the model parameters κ_s and m_s .

Instead of analytic method we use the code MicrOMEGAs [38] to calculate the s scalar relic density $\Omega_s h^2$, with the Feynman rules generated by the package LanHEP 3.2.0 [39]. In Fig.3 we project the contour of relic density $\Omega_s h^2$ as required by Eq.(4.1) to the two-parameter plane of (m_s, κ_s) . As expected the required value of κ_s is minimal for m_s near

$m_h/2$, because near this mass region the annihilation cross section is resonantly enhanced. Plot similar to Fig.3 is also shown, e.g., in [21]⁴.

Fig.3 indicates that a wide mass range for s scalar is viable. However, it also shows that κ_s bigger than 0.1 is required when m_s is far away from the *resonant mass region*. For example, large $\kappa_s \geq 0.5$ is needed for m_s above 3 TeV, which is not favored neither by the EW vacuum stability nor the perturbative analysis. In the next subsection, we discuss the direct detection in the allowed parameter space.

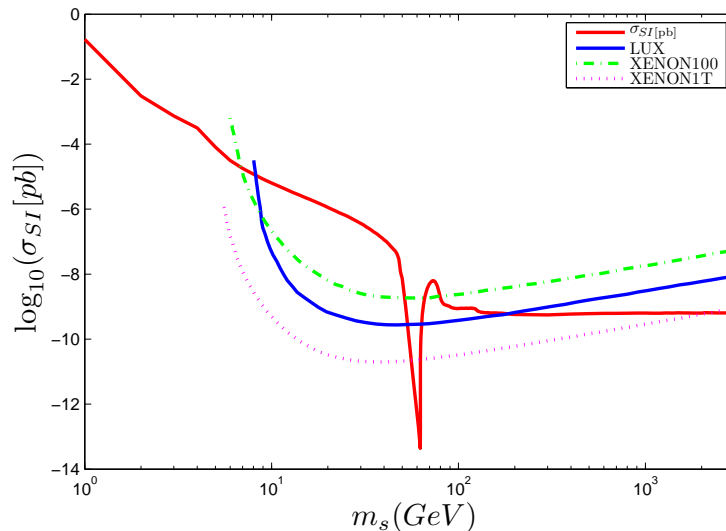


Figure 4: Spin-independent nucleon-DM scattering cross section as function of m_s . Various experimental limits are also shown for comparison.

4.2 Direct Detection

The spin-independent nucleon-DM scattering cross section is given by,

$$\sigma_{\text{SI}} = \frac{\kappa_s^2 f_N^2 \mu^2 m_N^2}{4\pi m_h^4 m_s^2}, \quad (4.2)$$

where m_N is the nucleon mass, $\mu = m_s m_N / (m_s + m_N)$ is the DM-nucleon reduced mass, and $f_N \sim 0.3$ [21] is the hadron matrix element.

⁴ Although these plots match very well, we would like to mention that contributions to σ_{ann} due to three- and four-body final states or QCD corrections are not included in MicrOMEGAs, with which the shape around W boson mass is smoother [40]. We thank the referee for reminding us this point. Since DM mass region near 80 GeV has been excluded by the LUX experiment, these corrections are expected to not affect our main results in Sec.6.

The current best limit on σ_{SI} comes from the Xenon100 [23] and LUX [25] experiments. In Fig.4 we plot the spin-independent nucleon-DM scattering cross section as function of m_s , with various experimental limits for comparison. The red curve corresponds to the DM relic density, which indicates that there are three viable regions,

$$\begin{aligned} \text{low mass region} & : 1 \text{ GeV} \leq m_s \leq 6 \text{ GeV}, \\ \text{resonant mass region} & : 56 \text{ GeV} \leq m_s \leq 66 \text{ GeV}, \\ \text{high mass region} & : m_s \geq 185 \text{ GeV}. \end{aligned} \tag{4.3}$$

By combining the constraint from SM vacuum stability, one finds that

- The *resonant mass region* is totally excluded, which is more powerful than the indirect constraint from the Fermi-LAT [27].
- The *high mass region* is further reduced to more narrow mass window, which is the subject of Xenon 1T [24] experiment for m_s below 4 TeV.
- The *low mass region* can be consistent with the constraint from SM vacuum stability. However, we will show in Sec.V that the *low mass region* is excluded by the Higgs invisible decay $h \rightarrow ss$ at the LHC experiment (see also some literature in Refs.[8-18]).

5 LHC Phenomenology

Since the scalar singlet only couples to the Higgs directly, the signal searches for this scalar at the LHC mainly focus on the Higgs invisible decay $h \rightarrow ss$ in the *low mass region* and *resonant mass region* with $m_s < m_h/2$. Note that for scalar singlet DM there is no mixing effect ⁵ between s and h , as clearly shown in Eq.(2.1) and Eq.(2.2).

Very recently, the ATLAS Collaboration has reported the latest data about the upper bound on the Higgs invisible decay width [26],

$$\Gamma_{\text{inv}} \leq 0.29 \Gamma_{\text{SM}}, \tag{5.1}$$

⁵If s scalar is not DM, one may discuss its phenomenology by introducing mixing effects. For a recent discussion, see [44].

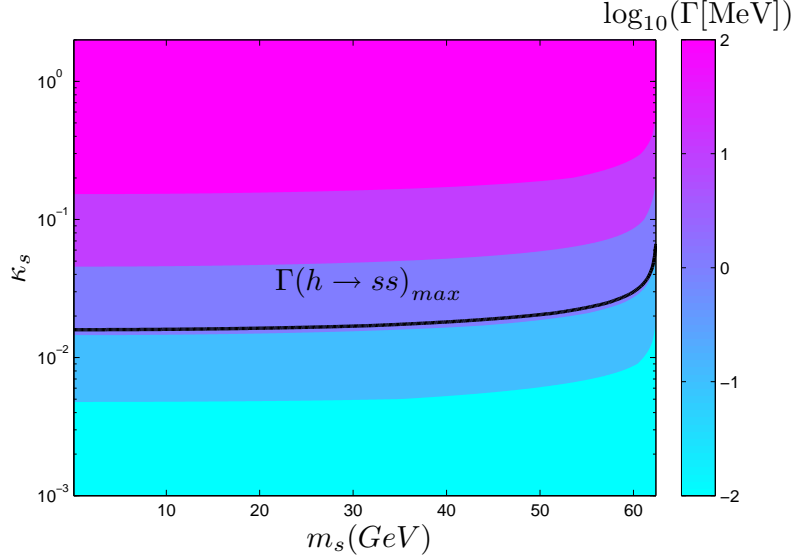


Figure 5: Contours of invisible decay width $\Gamma(h \rightarrow ss)$ in the two-parameter plane of $m_s - \kappa_s$. The contour in black denotes the latest upper bound in Eq.(5.1). Region above this line is excluded.

which is obviously stronger than what was used in some earlier literature. An update is thus meaningful. In Eq.(5.1) $\Gamma_{\text{SM}} \simeq 4.15$ MeV for 125 GeV Higgs mass, and the invisible decay width Γ_{inv} is given by,

$$\Gamma(h \rightarrow ss) = \frac{\kappa_s^2 v^2}{32\pi m_h} \sqrt{1 - \frac{4m_s^2}{m_h^2}}. \quad (5.2)$$

We show the decay width $\Gamma(h \rightarrow ss)$ in Fig.5. The contour in black denotes the latest upper bound in Eq.(5.1), and region above it is excluded. In particular, this bound excludes the whole *low mass region* and the *resonant mass region* with $m_s \leq 62.5$ GeV in Eq.(4.3). In contrast, the *high mass region* is less constrained at the LHC in compared with the *low mass region*.

6 Conclusions and Discussions

In this paper we have reconsidered the simplest HDM. By combining the constraints arising from DM relic density, direct detection limit on spin-independent nucleon-DM scattering cross section from the LUX, and limit on the Higgs invisible decay from the

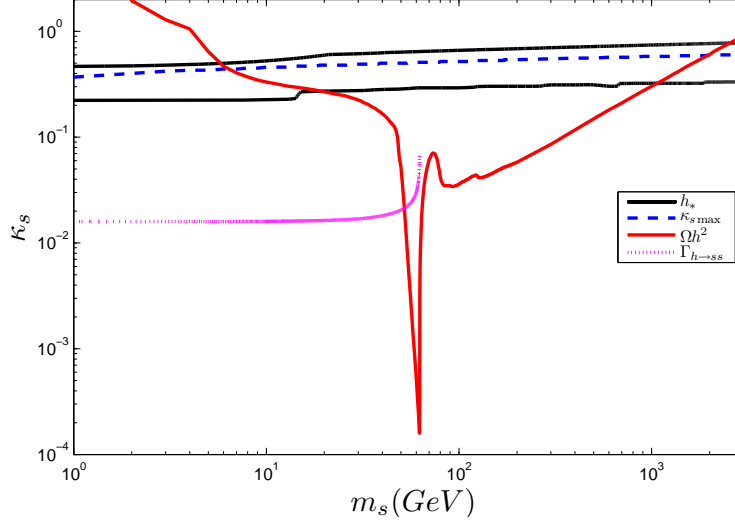


Figure 6: Mass regions consistent with various constraints. In the light of the SM vacuum stability, only mass region $1.1 \text{ TeV} \leq m_s \leq 2.5 \text{ TeV}$ is viable, and it slightly reduces to $1.1 \text{ TeV} \leq m_s \leq 2.0 \text{ TeV}$ by the additional requirement of perturbativity. For the explanation about h_* and $\kappa_{s\text{max}}$, see previous discussions.

LHC, we have obtained two viable mass regions (see Fig.6):

$$\begin{aligned} \text{resonant mass region} &: 62.5 \text{ GeV} \leq m_s \leq 66 \text{ GeV}, \\ \text{high mass region} &: m_s \geq 185 \text{ GeV}. \end{aligned} \quad (6.1)$$

We also show that if the constraint from the SM vacuum stability is imposed, we arrive at the main conclusion- the *resonant mass region* is totally excluded and the *high mass region* in Eq.(6.1) is reduced to a narrow window,

$$\text{high mass region} : 1.1 \text{ TeV} \leq m_s \leq 2.55 \text{ TeV}, \quad (6.2)$$

as shown in Fig.6. If one further imposes the constraint due to perturbativity, the mass range in Eq.(6.2) is slightly reduced to,

$$\text{high mass region} : 1.1 \text{ TeV} \leq m_s \leq 2.0 \text{ TeV}. \quad (6.3)$$

Fortunately, as shown in Fig.4 the mass region in Eq.(6.3) can be totally detected by the Xenon 1T experiment in the near future. Similarly to Xenon 1T experiment, this *high mass region* can be also directly detected at colliders in principle. As a result of

small production cross section of order less than 1 fb for the s scalar at the 14-TeV LHC [19], a 5σ discovery acquires luminosity at least of order $\mathcal{O}(10) \text{ ab}^{-1}$.

Independently, effects on large scale structure induced by DM self-interaction is a new window for the detection. In compared with the abelian vector- or fermion-like DM, s scalar with quartic self-interaction is very distinctive. DM self-interaction has been used to interpret [47] the observations on four galaxies in the core of galaxy cluster Abell 3827 [46]. If the new observations indeed arise from the DM self-interaction other than astrophysical artifact, the *high mass region* is highly constrained, see, e.g., for recent discussion [48].

In variety of contexts the *high mass region* in Eq.(6.2) may be modified. For example, it can be relaxed if one employs additional mechanism to stabilize the SM vacuum by introducing more new parameters, such as the non-minimal interaction between the Higgs and Ricci scalar with non-negligible coupling constant. In contrast, this *high mass region* may be alternatively strengthened if one assumes [21] that the DM relic abundance is partially other than totally saturated by the scalar singlet. In this case scalar s may play a positive role in the electroweak baryogenesis [40].

Acknowledgments

HH would like to thank Felix Kahlhoefer for suggesting the use of code LanHEP. This work is supported in part by the Natural Science Foundation of China under grant No.11247031 and 11405015.

References

- [1] G. Aad *et al.* [ATLAS Collaboration], “Combined search for the Standard Model Higgs boson using up to 4.9 fb^{-1} of pp collision data at $\sqrt{s} = 7 \text{ TeV}$ with the ATLAS detector at the LHC,” Phys. Lett. B **710**, 49 (2012), arXiv:1202.1408 [hep-ex].
- [2] S. Chatrchyan *et al.* [CMS Collaboration], “Combined results of searches for the standard model Higgs boson in pp collisions at $\sqrt{s} = 7 \text{ TeV}$,” Phys. Lett. B **710**, 26 (2012), arXiv:1202.1488 [hep-ex].
- [3] V. Silveira and A. Zee, “Scalar Phantoms,” Phys. Lett. B **161**, 136 (1985).

- [4] J. McDonald, “Gauge singlet scalars as cold dark matter,” *Phys. Rev. D* **50**, 3637 (1994), [hep-ph/0702143].
- [5] J. McDonald, “Thermally generated gauge singlet scalars as selfinteracting dark matter,” *Phys. Rev. Lett.* **88**, 091304 (2002). [hep-ph/0106249].
- [6] M. C. Bento, O. Bertolami, R. Rosenfeld and L. Teodoro, “Selfinteracting dark matter and invisibly decaying Higgs,” *Phys. Rev. D* **62**, 041302 (2000), [astro-ph/0003350].
- [7] C. P. Burgess, M. Pospelov and T. ter Veldhuis, “The Minimal model of nonbaryonic dark matter: A Singlet scalar,” *Nucl. Phys. B* **619**, 709 (2001), [hep-ph/0011335].
- [8] H. Davoudiasl, R. Kitano, T. Li and H. Murayama, “The New minimal standard model,” *Phys. Lett. B* **609**, 117 (2005), [hep-ph/0405097].
- [9] A. Kusenko, “Sterile neutrinos, dark matter, and the pulsar velocities in models with a Higgs singlet,” *Phys. Rev. Lett.* **97**, 241301 (2006), [hep-ph/0609081].
- [10] D. O’Connell, M. J. Ramsey-Musolf and M. B. Wise, “Minimal Extension of the Standard Model Scalar Sector,” *Phys. Rev. D* **75**, 037701 (2007), [hep-ph/0611014].
- [11] V. Barger, P. Langacker, M. McCaskey, M. J. Ramsey-Musolf and G. Shaughnessy, “LHC Phenomenology of an Extended Standard Model with a Real Scalar Singlet,” *Phys. Rev. D* **77**, 035005 (2008), arXiv:0706.4311 [hep-ph].
- [12] H. Sung Cheon, S. K. Kang and C. S. Kim, “Low Scale Leptogenesis and Dark Matter Candidates in an Extended Seesaw Model,” *JCAP* **0805**, 004 (2008), [*JCAP* **1103**, E01 (2011)], arXiv:0710.2416 [hep-ph].
- [13] X. G. He, T. Li, X. Q. Li, J. Tandean and H. C. Tsai, “Constraints on Scalar Dark Matter from Direct Experimental Searches,” *Phys. Rev. D* **79** (2009) 023521, arXiv:0811.0658 [hep-ph].
- [14] R. N. Lerner and J. McDonald, “Gauge singlet scalar as inflaton and thermal relic dark matter,” *Phys. Rev. D* **80**, 123507 (2009), arXiv:0909.0520 [hep-ph].
- [15] M. Farina, D. Pappadopulo and A. Strumia, “CDMS stands for Constrained Dark Matter Singlet,” *Phys. Lett. B* **688** (2010) 329, arXiv:0912.5038 [hep-ph].

- [16] W. L. Guo and Y. L. Wu, “The Real singlet scalar dark matter model,” JHEP **1010** (2010) 083, arXiv:1006.2518 [hep-ph].
- [17] S. Profumo, L. Ubaldi and C. Wainwright, “Singlet Scalar Dark Matter: monochromatic gamma rays and metastable vacua,” Phys. Rev. D **82** (2010) 123514, arXiv:1009.5377 [hep-ph].
- [18] A. Biswas and D. Majumdar, “The Real Gauge Singlet Scalar Extension of Standard Model: A Possible Candidate of Cold Dark Matter,” Pramana **80**, 539 (2013), arXiv:1102.3024 [hep-ph].
- [19] A. Djouadi, O. Lebedev, Y. Mambrini and J. Quevillon, “Implications of LHC searches for Higgs–portal dark matter,” Phys. Lett. B **709**, 65 (2012), arXiv:1112.3299 [hep-ph].
- [20] A. Djouadi, A. Falkowski, Y. Mambrini and J. Quevillon, “Direct Detection of Higgs–Portal Dark Matter at the LHC,” Eur. Phys. J. C **73** (2013) 2455, arXiv:1205.3169 [hep-ph].
- [21] J. M. Cline, K. Kainulainen, P. Scott and C. Weniger, “Update on scalar singlet dark matter,” Phys. Rev. D **88** (2013) 055025, arXiv:1306.4710 [hep-ph].
- [22] P. A. R. Ade *et al.* [Planck Collaboration], “Planck 2013 results. XVI. Cosmological parameters,” Astron. Astrophys. **571**, A16 (2014). arXiv:1303.5076 [astro-ph.CO].
- [23] E. Aprile *et al.* [XENON100 Collaboration], “Dark Matter Results from 225 Live Days of XENON100 Data,” Phys. Rev. Lett. **109**, 181301 (2012), arXiv:1207.5988 [astro-ph.CO].
- [24] E. Aprile *et al.* [XENON1T Collaboration], “The XENON1T Dark Matter Search Experiment,” arXiv:1206.6288 [astro-ph.IM].
- [25] D. S. Akerib *et al.* [LUX Collaboration], “First results from the LUX dark matter experiment at the Sanford Underground Research Facility,” Phys. Rev. Lett. **112**, 091303 (2014), arXiv:1310.8214 [astro-ph.CO].
- [26] G. Aad *et al.* [ATLAS Collaboration], “Search for an Invisibly Decaying Higgs Boson Produced via Vector Boson Fusion in pp Collisions at $\sqrt{s} = 8$ TeV using the ATLAS detector at the LHC,” ATLAS-CONF-2015-004.

- [27] M. Ackermann *et al.* [Fermi-LAT Collaboration], “Search for gamma-ray spectral lines with the Fermi large area telescope and dark matter implications,” *Phys. Rev. D* **88**, 082002 (2013), arXiv:1305.5597 [astro-ph.HE].
- [28] L. Feng, S. Profumo and L. Ubbaldi, “Closing in on singlet scalar dark matter: LUX, invisible Higgs decays and gamma-ray lines,” *JHEP* **1503**, 045 (2015), arXiv:1412.1105 [hep-ph].
- [29] M. Duerr, P. F. Perez, J. Smirnov, “Scalar Singlet Dark Matter and Gamma Lines,” arXiv:1508.04418 [hep-ph].
- [30] C. E. Yaguna, “Gamma rays from the annihilation of singlet scalar dark matter,” *JCAP* **0903**, 003 (2009), arXiv:0810.4267 [hep-ph].
- [31] D. Buttazzo, G. Degrandi, P. P. Giardino, G. F. Giudice, F. Sala, A. Salvio and A. Strumia, “Investigating the near-criticality of the Higgs boson,” *JHEP* **1312**, 089 (2013), arXiv:1307.3536 [hep-ph].
- [32] A. Kobakhidze and A. Spencer-Smith, “Electroweak Vacuum (In)Stability in an Inflationary Universe,” *Phys. Lett. B* **722**, 130 (2013), arXiv:1301.2846 [hep-ph].
- [33] A. Hook, J. Kearney, B. Shakya and K. M. Zurek, “Probable or Improbable Universe? Correlating Electroweak Vacuum Instability with the Scale of Inflation,” *JHEP* **1501**, 061 (2015), arXiv:1404.5953 [hep-ph].
- [34] J. R. Espinosa, G. F. Giudice, E. Morgante, A. Riotto, L. Senatore, A. Strumia and N. Tetradis, “The cosmological Higgstory of the vacuum instability,” arXiv:1505.04825 [hep-ph].
- [35] N. Khan and S. Rakshit, “Study of electroweak vacuum metastability with a singlet scalar dark matter,” *Phys. Rev. D* **90**, no. 11, 113008 (2014), arXiv:1407.6015 [hep-ph].
- [36] M. Kadastik, K. Kannike, A. Racioppi and M. Raidal, “Implications of the 125 GeV Higgs boson for scalar dark matter and for the CMSSM phenomenology,” *JHEP* **1205**, 061 (2012), arXiv:1112.3647 [hep-ph].
- [37] F. Kahlhoefer and J. McDonald, “WIMP Dark Matter and Unitarity-Conserving Inflation via a Gauge Singlet Scalar,” arXiv:1507.03600 [astro-ph.CO].

- [38] G. Belanger, F. Boudjema, A. Pukhov and A. Semenov, “micrOMEGAs4.1: two dark matter candidates,” *Comput. Phys. Commun.* **192**, 322 (2015), arXiv:1407.6129 [hep-ph].
- [39] A. Semenov, “LanHEP - a package for automatic generation of Feynman rules from the Lagrangian. Updated version 3.2,” arXiv:1412.5016 [physics.comp-ph].
- [40] J. M. Cline and K. Kainulainen, “Electroweak baryogenesis and dark matter from a singlet Higgs,” *JCAP* **1301**, 012 (2013), arXiv:1210.4196 [hep-ph].
- [41] C. Cheung, M. Papucci and K. M. Zurek, “Higgs and Dark Matter Hints of an Oasis in the Desert,” *JHEP* **1207**, 105 (2012), arXiv:1203.5106 [hep-ph].
- [42] S. Zheng, “Can Higgs Inflation be Saved with High-scale Supersymmetry ?,” *Eur. Phys. J. C* **75** (2015) 489, arXiv:1504.08093 [hep-ph].
- [43] J. R. Espinosa, G. F. Giudice and A. Riotto, *JCAP* **0805**, 002 (2008), arXiv:0710.2484 [hep-ph].
- [44] S. Zheng, “Discovery of Scalar Mixed With SM Higgs Via Diboson Excess at the LHC,” arXiv:1508.06014 [hep-ph].
- [45] R. Campbell, S. Godfrey, H. E. Logan, A. D. Peterson and A. Poulin, “Implications of the observation of dark matter self-interactions for singlet scalar dark matter,” arXiv:1505.01793 [hep-ph].
- [46] R. Massey *et al.*, “The behaviour of dark matter associated with four bright cluster galaxies in the 10 kpc core of Abell 3827,” *Mon. Not. Roy. Astron. Soc.* **449**, no. 4, 3393 (2015), arXiv:1504.03388 [astro-ph.CO].
- [47] F. Kahlhoefer, K. Schmidt-Hoberg, J. Kummer and S. Sarkar, “On the interpretation of dark matter self-interactions in Abell 3827,” *Mon. Not. Roy. Astron. Soc.* **452**, 1 (2015), arXiv:1504.06576 [astro-ph.CO].
- [48] R. Campbell, S. Godfrey, H. E. Logan, A. D. Peterson and A. Poulin, “Implications of the observation of dark matter self-interactions for singlet scalar dark matter,” arXiv:1505.01793 [hep-ph].